Molecular Therapy
Nucleic Acids
Original Article

Silencing of lncRNA LINC00857 Enhances BIRC5-Dependent Radio-Sensitivity of Lung Adenocarcinoma Cells by Recruiting NF-κB1

Fushi Han,[1] Shusong Yang,[2] Wei Wang,[3] Xinghong Huang,[4] Dongdong Huang,[5] and Shuzhen Chen[1]

[1]Department of Nuclear Medicine, Tongji Hospital, Tongji University School of Medicine, Shanghai 200065, P.R. China; [2]Department of Radiotherapy, Tongji Hospital, Tongji University School of Medicine, Shanghai 200065, P.R. China; [3]Department of Internal Medicine, Tongji Hospital, Tongji University School of Medicine, Shanghai 200065, P.R. China; [4]Department of Radiology, Tongji Hospital, Tongji University School of Medicine, Shanghai 200065, P.R. China; [5]Department of Emergency Medicine, Shanghai Pulmonary Hospital, Tongji University School of Medicine, Shanghai 200433, P.R. China

Lung adenocarcinoma (LUAD) is a predominant type of lung cancer in never-smoker patients. In this study, we identified a long noncoding RNA (lncRNA) LINC00857 that might regulate radio-sensitivity of LUAD cells. Expression of LINC00857 and baculoviral IAP repeat containing 5 (BIRC5) was determined to be upregulated in LUAD cells and tissues using qRT-PCR and western blot analysis. The correlation between LINC00857 and nuclear factor kappa B subunit 1 (NF-κB1) was verified using RNA immunoprecipitation and chromatin immunoprecipitation assays, while the binding relationship between NF-κB1 and BIRC5 was determined by dual-luciferase reporter assay. It was suggested that LINC00857 could recruit NF-κB1 in BIRC5 promoter region. BIRC5 promoter activity was repressed in response to small interfering-LINC00857 (si-LINC00857) in LUAD cells. Silencing LINC00857 or BIRC5 reduced proliferation and colony formation but enhanced apoptosis and radio-sensitivity of LUAD cells. The experiment *in vivo* verified the function of silencing LINC00857 on enhancing radio-sensitivity of LUAD cells. Our results reveal a functional regulatory LINC00857-NF-κB1-BIRC5 triplet in LUAD cells, suggesting LINC00857 as a potential target for LUAD treatment.

INTRODUCTION

Lung adenocarcinoma (LUAD), as the most common subtype of lung cancer, is a major cause of cancer mortality worldwide.[1] Despite its deficiencies, radiotherapy remains the most commonly applied therapy for early-stage LUAD patients.[2] Recently, the technique of RNA sequencing of single tumor cells offers a comprehensive understanding of gene candidates related to anti-tumor drug response which facilitates the development of optimized clinical anti-tumor therapeutics.[3] Long noncoding RNAs (lncRNAs) play a pivotal role in carcinogenesis, tumor invasion, and metastasis.[4,5] For example, lncRNA CASC9.5 was reported to be a tumor-promoting gene in the proliferation and metastasis of LUAD.[6] Furthermore, lncRNAs can affect radio-sensitivity in LUAD. For instance, CRNDE could reduce the radio-sensitivity and apoptosis of LUAD cells via targeting p21.[7] Hence, identification of therapeutically relevant molecular mechanisms in LUAD may aid in developing more effective anti-tumor therapies.

LINC00857 exhibits prognostic potential for poor patient survival and promotes the development of lung cancer by mediating the cell cycle.[8] A recent study showed that LINC00857 facilitates the progression of LUAD by modulating the miR-1179/SPAG5 axis;[9] however, the radio-sensitivity-associated mechanism remains unknown. Conceivably, lncRNAs could bind to histone-modifying complexes, DNA binding proteins (such as transcription factors) and RNA polymerase II to modulate the transcriptional process.[10] In this study, we focused on the LINC00857-NF-κB1-BIRC5 triplet of LUAD, which was predicted by the LncMap database (http://bio-bigdata.hrbmu.edu.cn/LncMAP/index.jsp). Baculoviral IAP repeat-containing 5 (BIRC5) is already acknowledged as a cancer therapy-resistance factor,[11] and BIRC5 expression was elevated in non-small cell lung cancer samples.[12] Another study noted a promotive role of BIRC5 in the development of lung cancer,[13] and a more recent study identified BIRC5 to be one of top hub genes in LUAD based on bioinformatics.[14] More specifically, nuclear factor kappa B subunit 1 (NF-κB1), an important transcription factor in many pathways, functioned as a suppressor of inflammation, aging, and cancer.[15] Thus, we proposed a hypothesis that LINC00857 mediated radio-sensitivity of LUAD by regulating BIRC5 via NF-κB1. To test this hypothesis, we explored the regulatory mechanism of the LINC00857/BIRC5/NF-κB1 axis in LUAD.

RESULTS

Expression of BIRC5 and LINC00857 in LUAD by Microarray-Based Analysis

BIRC5 was found to be upregulated in specimens from LUAD patients using the UALCAN website (http://ualcan.path.uab.edu/

Received 5 March 2020; accepted 17 September 2020;
https://doi.org/10.1016/j.omtn.2020.09.020.

Correspondence: Shuzhen Chen, Department of Nuclear Medicine, Tongji Hospital, Tongji University School of Medicine, No. 389, Xincun Road, Putuo District, Shanghai 200065, P.R. China.
E-mail: alice3396@126.com

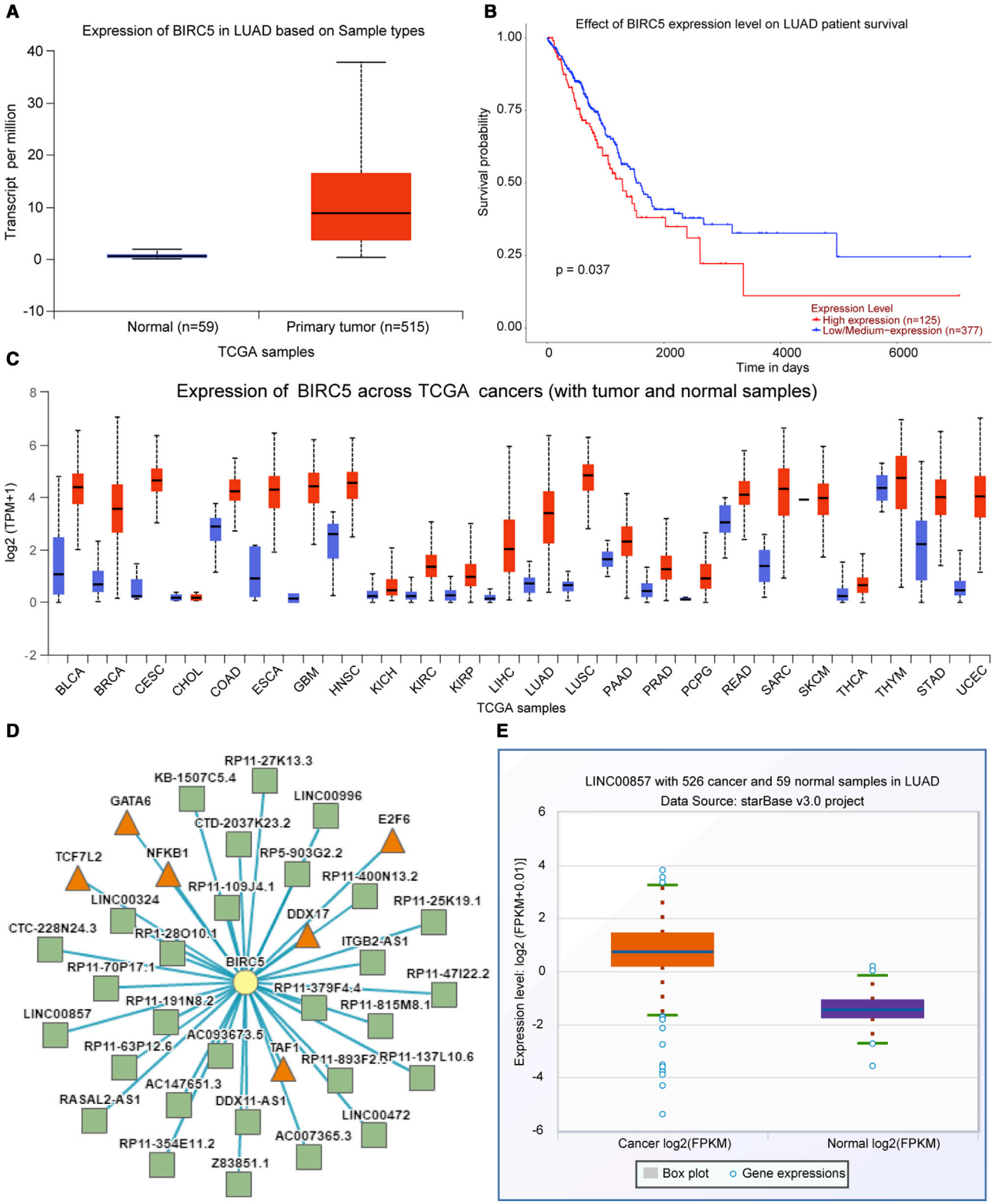

(legend on next page)

Table 1. lncRNA-TF-Gene Triplet

Cancer Type	lncRNA Symbol	TF Symbol	Gene Symbol
LUAD	RP11-25K19.1	NFKB1	BIRC5
LUAD	LINC00324	NFKB1	BIRC5
LUAD	RP11-137L10.6	DDX17	BIRC5
LUAD	AC147651.3	DDX17	BIRC5
LUAD	RASAL2-AS1	NFKB1	BIRC5
LUAD	RP11-63P12.6	TCF7L2	BIRC5
LUAD	RP11-70P17.1	TAF1	BIRC5
LUAD	AC007365.3	E2F6	BIRC5
LUAD	ITGB2-AS1	TAF1	BIRC5
LUAD	RP1-28O10.1	TAF1	BIRC5
LUAD	RP11-191N8.2	E2F6	BIRC5
LUAD	RP11-400N13.2	E2F6	BIRC5
LUAD	Z83851.1	NFKB1	BIRC5
LUAD	AC093673.5	NFKB1	BIRC5
LUAD	LINC00472	TCF7L2	BIRC5
LUAD	RP11-354E11.2	TAF1	BIRC5
LUAD	RP11-27K13.3	E2F6	BIRC5
LUAD	LINC00857	NFKB1	BIRC5
LUAD	RP11-815M8.1	E2F6	BIRC5
LUAD	RP11-379F4.4	GATA6	BIRC5

LUAD, lung adenocarcinoma; BIRC5, baculoviral IAP repeat containing 5; NF-κB1, nuclear factor kappa B subunit 1

analysis.html; Figure 1A), and Kaplan-Meier analysis of the patient survival curve (Figure 1B) indicated that BIRC5 expression was associated with the LUAD patient survival. Meanwhile, BIRC5 was also found to be elevated in other tumors (Figure 1C). BIRC5 was identified in the lncRNA-transcription factor (TF)-gene triplet of LUAD by the LncMap program (http://bio-bigdata.hrbmu.edu.cn/LncMAP/index.jsp; Figure 1D; Table 1). As shown in Figure 1E, LINC00857 expression was elevated in LUAD following analysis using the Starbase dataset.

LINC00857 Was Overexpressed in LUAD Tissues and Cells

As shown in Figure 2A, results of quantitative reverse transcription polymerase chain reaction (qRT-PCR) analysis displayed that LINC00857 expression was higher in LUAD tissues than in normal tissues. Moreover, LINC00857 expression closely correlated with tumor diameter, differentiation, and tumor node metastasis (TNM) stage ($p < 0.05$), but had no relationship with differences in age, gender, and lymph node metastasis ($p > 0.05$; Table 2). Kaplan-Meier analysis further identified that the overall survival time was remarkably shorter in LUAD patients with elevated LINC00857 expression (Figure 2B, $p < 0.05$). According to qRT-PCR, LINC00857 was upregulated in 4 lung cancer cell lines as compared to that in Beas-2B human pulmonary epithelial cells (Figure 2C, $p < 0.05$). LUAD cell line A549 with the highest LINC00857 expression was selected for subsequent experiments. The Cell Counting Kit-8 (CCK-8) assay (Figure 2D) demonstrated that the cell viability was reduced with increasing radiation dose. There was a 50% reduction in LUAD cell viability at a dose of 6.0 Gy; this dose was chosen for further experiments.

Silencing of LINC00857 Enhanced Radio-Sensitivity in LUAD Cells

Subsequently, a small interfering RNA (siRNA) against LINC00857 (si-LINC00857) was designed to knockdown LINC00857. The silencing efficiency of si-LINC00857 in A549 cells, which were radiated under 0 and 6.0 Gy γ-irradiation, was measured by qRT-PCR. As shown in Figure 3A, LINC00857 expression was considerably reduced after treatment of si-LINC00857. After transfection, CCK-8, flow cytometry and colony formation assays (Figures 3B–3D) were carried out, and the results exhibited significantly reduced proliferation and colony formation but enhanced apoptosis with LINC00857 silencing in the cells treated with 6.0 Gy irradiation ($p < 0.05$). In contrast, there was no significant change in A549 cells under 0 Gy irradiation ($p > 0.05$). Western blot analysis (Figure 3E) revealed significantly decreased protein expression of Ki67, proliferating-cell-nuclear-antigen (PCNA), and Bcl-2 and increased Bax expression in the A549 cells upon LINC00857 silencing ($p < 0.05$).

Additionally, we conducted experiments in the H2444 cells to validate the effect of si-LINC00857. qRT-PCR confirmed the silencing efficiency of si-LINC00857 in the H2444 cells (Figure S1A). The results of CCK-8 assay (Figure S1B) suggested that LINC00857 silencing contributed to noticeable suppression in viability of the H2444 cells irradiated by 6.0 Gy ($p < 0.05$), corresponding to reductions in Ki67, PCNA, and Bcl-2 and an elevation in Bax expression ($p < 0.05$) (Figure S1C). However, no substantial changes were witnessed in H2444 cells under 0 Gy irradiation ($p > 0.05$). Taken together, silencing of LINC00857 enhanced radio-sensitivity of LUAD cells under 6.0 Gy irradiation.

LINC00857 Elevates BIRC5 Expression by Recruiting NF-κB1

The LncMAP database predicted that LINC00857 might regulate BIRC5 expression through transcription factor NF-κB1 in LUAD (Figure 4A). qRT-PCR (Figure 4B) confirmed upregulation of BIRC5 in LUAD tissues and the A549 cell line ($p < 0.05$). Western blot analysis (Figure 4C) revealed a substantial reduction of BIRC5

Figure 1. Expression Patterns of BIRC5 and LINC00857 in LUAD

(A) BIRC5 expression in LUAD patients predicted using UALCAN; abscissa indicates sample types, while ordinate indicates BIRC5 expression. (B) Patients survival curve using Kaplan-Meier method. (C) BIRC5 expression in other tumors; blue represents normal samples, while red represents tumor sample. (D) BIRC5 was identified in the lncRNA-TF-gene triplet of LUAD using LncMap. The square symbol represents lncRNA, the triangle represents TF, and the circle represents the different genes. (E) Starbase prediction of LINC00857 expression in LUAD; abscissa represents sample types, while ordinate indicates LINC00857 expression.

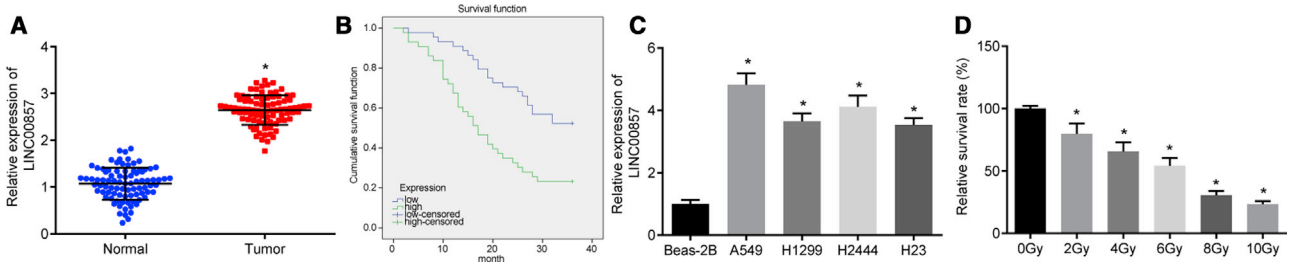

Figure 2. LINC00857 Was Highly Expressed in LUAD Tissues and Cells

(A) LINC00857 expression in LUAD tissues and normal tissues determined by qRT-PCR, *p < 0.05 versus adjacent normal tissues, n = 87; (B) The overall survival of LUAD patients with high and low LINC00857 expression plotted by the Kaplan-Meier method. (C) LINC00857 expression in pulmonary epithelial cell line Beas-2B and 4 lung cancer cell lines determined by qRT-PCR, *p < 0.05 versus Beas-2B cells; the cell experiment was conducted independently in triplicate. (D) LUAD cell viability tested after radiation at different doses using CCK-8. *p < 0.05 versus 0 Gy, the cell experiments were conducted three times independently. Measurement data were expressed as mean ± standard deviation and analyzed by unpaired t test. Differences among multiple groups were analyzed by one-way ANOVA. Log-rank test was performed to analyze the survival time.

protein expression in response to LINC00857 silencing, but an increase of BIRC5 protein expression in the LUAD cells overexpressing LINC00857 ($p < 0.05$). The binding of LINC00857 to NF-κB1 was verified using RNA immunoprecipitation (RIP; Figure 4D), which showed an enrichment of LINC00857 co-precipitated with NF-κB1 ($p < 0.05$). The dual-luciferase reporter assay (Figure 4E) was adopted to determine the effect of NF-κB1 on BIRC5 promoter. The luciferase activity of wild-type (WT)-BIRC5 was markedly reduced by co-treatment with si-NF-κB1 ($p < 0.05$), while no significant changes were observed in the luciferase activity of mut-BIRC5 ($p > 0.05$). The binding relationship between NF-κB1 and BIRC5 was further clarified by chromatin immunoprecipitation (ChIP; Figure 4F). The results revealed that compared to immunoglobulin G (IgG), BIRC5 enrichment was increased in the NF-κB1 group, and a significant BIRC5 enrichment was also seen after LINC00857 silencing ($p < 0.05$).

To better elucidate whether LINC00857, NF-κB1, and BIRC5 interact with each other, we conducted qRT-PCR to measure the expression of LINC00857, NF-κB1, and BIRC5 after alteration of LINC00857. Silencing of LINC00857 caused significant decreased BIRC5 expression but had no effect on the expression of NF-κB1, whereas BIRC5 expression remained unchanged in response to NF-κB1 overexpression in the cells treated with si-LINC00857 (Figure 4G, $p < 0.05$). The results determined by western blot analysis (Figure 4H) shared similar changes in protein expression of NF-κB1 and BIRC5 with that in mRNA expression determined by qRT-PCR ($p < 0.05$). All of the above experiments suggested that LINC00857 could upregulate BIRC5 by recruiting NF-κB1.

LINC00857-NF-κB1-BIRC5 Triplet Regulated the Radio-Sensitivity in LUAD

Western blot analysis (Figure 5A) of BIRC5 protein expression in A549 cells revealed that BIRC5 protein expression was markedly upregulated in response to si-negative control (si-NC) and oe-BIRC5 co-treatment compared with cells co-treated with si-NC and oe-NC, and a similar increase in BIRC5 protein expression was observed in cells co-treated with si-LINC00857 and oe-BIRC5 treatment when compared with si-LINC00857 and oe-NC co-treatment. As shown in Figures 5B–5D, CCK-8, flow cytometry and colony formation assays were employed to measure A549 cell proliferation and apoptosis. It was illustrated that in cells irradiated by 6.0 Gy γ-ray, LINC00857 silencing considerably impaired A549 cell proliferation but promoted apoptosis, as evidenced by reduced cell viability and colony-formation rate, as well as increased apoptotic rate, while BIRC5 overexpression contributed to enhanced cell proliferation and reduced apoptosis. Moreover, BIRC5 overexpression counteracted the effects of LINC00857 silencing on A549 cell proliferation and apoptosis. However, there was no significant disparity after alteration of LINC00857 and BIRC5 expression in cells radiated by 0 Gy γ-ray ($p > 0.05$). Further, western blot analysis (Figure 5E) showed that LINC00857 silencing led to markedly decreased protein expression of Ki67, PCNA, and Bcl-2 but substantially increased protein levels of Bax. Overexpression of BIRC5 resulted in opposite changes in the levels of the aforementioned proteins, and reversed the changes induced by LINC00857 silencing ($p < 0.05$). Additionally, A549 cell line with mutant (MUT) p53 was generated by knocking down p53. The apoptosis of p53 WT or MUT A549 cells was assessed by flow cytometry, the results of which exhibited that A549 cell apoptosis under radiation at 6 Gy γ-ray was inhibited after p53 knockdown (Figure 5F). As measured by western blot analysis, BIRC5 protein expression was gradually increased in the A549 cells under radiation in a dose-dependent manner (Figure 5G). Above all, when irradiation dose was under 6.0 Gy γ-ray, silencing of LINC00857 enhanced the radio-sensitivity of LUAD cells via downregulating BIRC5.

Silencing of LINC00857 Impaired the LUAD Development and Enhanced the Radio-Sensitivity *In Vivo*

Finally, the *in vivo* tumorigenesis model was developed to verify the effect of LINC00857 on radio-sensitivity in tumor-bearing nude mice irradiated with 6.0 Gy γ-ray. As illustrated in Figures 6A–6C, qRT-PCR, tumor volume monitoring and immunohistochemistry results demonstrated that mice injected with cells stably infected with si-LINC00857 showed reductions in LINC00857 expression, tumor volume, and BIRC5-positive rate. By contrast, increases in

Table 2. The relationship between LINC00857 Expression Level and Clinicopathological Factors

Clinicopathological Factors	Cases	LINC00857 Mean ± Standard Deviation	p
Gender			0.844
male	56	2.640 ± 0.314	
female	31	2.654 ± 0.322	
Age (years)			0.953
≤45	46	2.647 ± 0.290	
>45	41	2.643 ± 0.345	
Tumor diameter (cm)			< 0.001
≤4	48	2.427 ± 0.225	
>4	39	2.914 ± 0.167	
Degree of tumor differentiation			0.006
low	17	2.804 ± 0.369	
medium	31	2.678 ± 0.297	
high	39	2.565 ± 0.287	
Lymph node metastasis			0.528
yes	28	2.676 ± 0.267	
no	59	2.630 ± 0.337	
TNM staging			<0.001
I	10	2.181 ± 0.390	
II	26	2.460 ± 0.114	
III	51	2.830 ± 0.202	

Measurement data were expressed as mean ± standard deviation and analyzed by unpaired t test and differences among multiple groups were analyzed by one-way ANOVA, followed by Tukey's post hoc test. $p < 0.05$ means statistically significant.

LINC00857 expression, tumor volume, and BIRC5-positive rate were observed in mice injected with LINC00857-overexpressed A549 cells ($p < 0.05$). These observations provided further evidence for the function of LINC00857 silencing in promoting the radio-sensitivity of LUAD cells *in vivo*.

DISCUSSION

Among most commonly diagnosed cancers worldwide, lung cancer remains a major cause of mortality.[16] Radiotherapy is the most common treatment for lung cancer, which reduces metastasis occurrence and provides a better local control.[17] The present study identified the inhibitory role of LINC00857 in the radiotherapy sensitivity of LUAD. Based on our findings, we concluded that downregulated LINC00857 repressed BIRC5 expression by inhibiting NF-κB1 enrichment in BIRC5 promoter, which hindered the LUAD cell proliferation as well as enhanced the radiotherapy sensitivity and apoptosis of LUAD cells.

Our study provided substantial evidence in relation to the notions that LINC00857 was upregulated in LUAD tissues and cells, and that silencing of LINC00857 enhanced the radio-sensitivity and apoptosis of LUAD cells as well as inhibited the LUAD cell proliferation. lncRNAs play pivotal regulatory functions and are emerging as new players in tumorigenesis and phenotypic exterminators of lung cancer.[18] Due to the regulatory role of lncRNAs in the tumorigenesis of lung cancer, investigations relevant to their functions in lung cancer were common in recent years. For example, lncRNA metastasis-associated lung adenocarcinoma transcript (MALAT1) was reported to be oncogenic in numerous cancers.[19] A more recent study suggested that lncRNAs were involved in lung adenocarcinoma and associated with the survival of patients.[20] Similarly, lncRNA DANCR repression was reported to inhibit invasion in LUAD cells.[21] Another study identified 281 lncRNAs with significant differential-expression in LUAD and further highlighted the role of LINC00857 as a diagnostic/prognostic biomarker in LUAD.[8] Accordingly, we found evidence implicating LINC00857 in LUAD tumorigenesis. Another recent study reported that LINC00857 facilitated the growth and glycolysis of LUAD cells and suppressed the apoptosis by inhibiting miR-1179 and upregulating SPAG5,[9] which suggests a competing endogenous RNA (ceRNA) mechanism underlying the role of LINC00857. Through LncMap prediction, we identified the LUAD associated LINC00857-NF-κB1-BIRC5 triplet. BIRC5 was found to be overexpressed in head and neck squamous cell carcinomas, which emerged as an acknowledged cancer therapy-resistance factor[11] and its regulatory role in colorectal cancer has also been previously noted.[22] The level of BIRC5 mRNA was elevated and served as a marker of malignant transformation in NSCLC.[12] Of note, LUAD patients with BIRC5 high expression were at higher risk of distal metastasis and advanced N stage.[23] BIRC5 is well known as a regulator to prevent apoptotic cell death that is associated with enhanced drug resistance of lung cancer cells,[24] especially radiation resistance.[25] Consistent with this, our current study also revealed that BIRC5 exerted anti-apoptotic effects on LUAD cells and contributed to reduction in the radio-sensitivity of LUAD cells.

Our findings showed that LINC00857 downregulation could significantly decrease protein expression of Ki67, PCNA, and Bcl-2, but substantially increased protein expression of Bax. Ki67 was linked to advanced tumor stage as a labeling index,[26] and other radio-sensitivity-related genes like PCNA tended to have similar effects in another study.[27] In addition, lower levels of Bcl-2 and higher levels of Bax predicted for enhanced radio-sensitivity.[28] Consistent with the previous results, silencing of LINC00857 contributed to restored radio-sensitivity. We further presented evidence that silencing of LINC00857 enhanced radio-sensitivity of LUAD cells *in vivo*. Furthermore, BIRC5 gain-of-

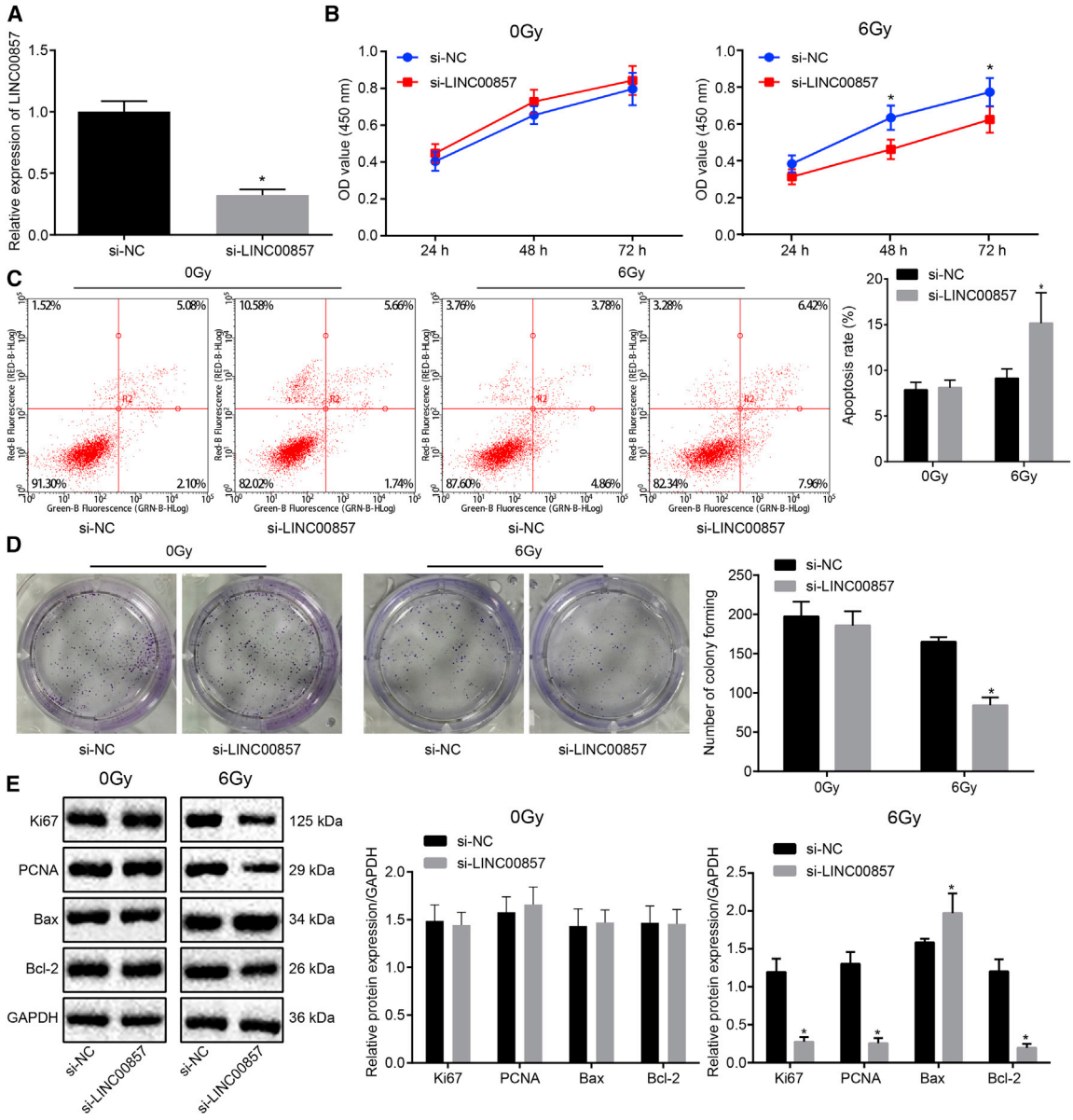

Figure 3. LINC00857 Knockdown Enhanced Radio-Sensitivity of A549 Cells

(A) Transfection efficiency measured by qRT-PCR. (B) Viability of A549 cells after LINC00857 knockdown tested using CCK-8. (C) Flow cytometric detection on A549 cell apoptosis after LINC00857 knockdown. (D) Colony formation ability of A549 cells after LINC00857 knockdown. (E) Western blot analysis of Ki67, PCNA, Bax, and Bcl-2 protein expression in A549 cells after LINC00857 knockdown. *$p < 0.05$ versus si-NC; measurement data were expressed as mean ± standard deviation and analyzed by unpaired t test. OD values at different time points were compared using two-way ANOVA. The cell experiments were conducted three times independently.

function reversed the effects of LINC00857 silencing on LUAD cellular behaviors and the expression of proliferation- and apoptosis-related proteins, demonstrating the mechanism whereby LINC00857 silencing enhanced radio-sensitivity of LUAD cells via downregulating BIRC5.

In the current study, we further demonstrated that LINC00857 could upregulate BIRC5 expression by recruiting NF-κB1, and then illustrated the regulatory role of the LINC00857-NF-κB1-BIRC5 triplet in the radio-sensitivity of LUAD. NF-κB1 has been previously noted as a promoter of radiation resistance.[29,30] Targeting NF-κB1 increased the sensitivity of tumor cells not only to chemotherapeutic agents but also to radiation exposure.[31] For example, inhibition of NF-κB1 by miR-9 and let-7g enhances the sensitivity of lung cancer cells to ionizing radiation.[32] Recently, suppression of NF-κB1 by its inhibitor IMD 0354 or p65 depletion was also shown to potentiate radio-sensitivity of lung cancer cells.[33]

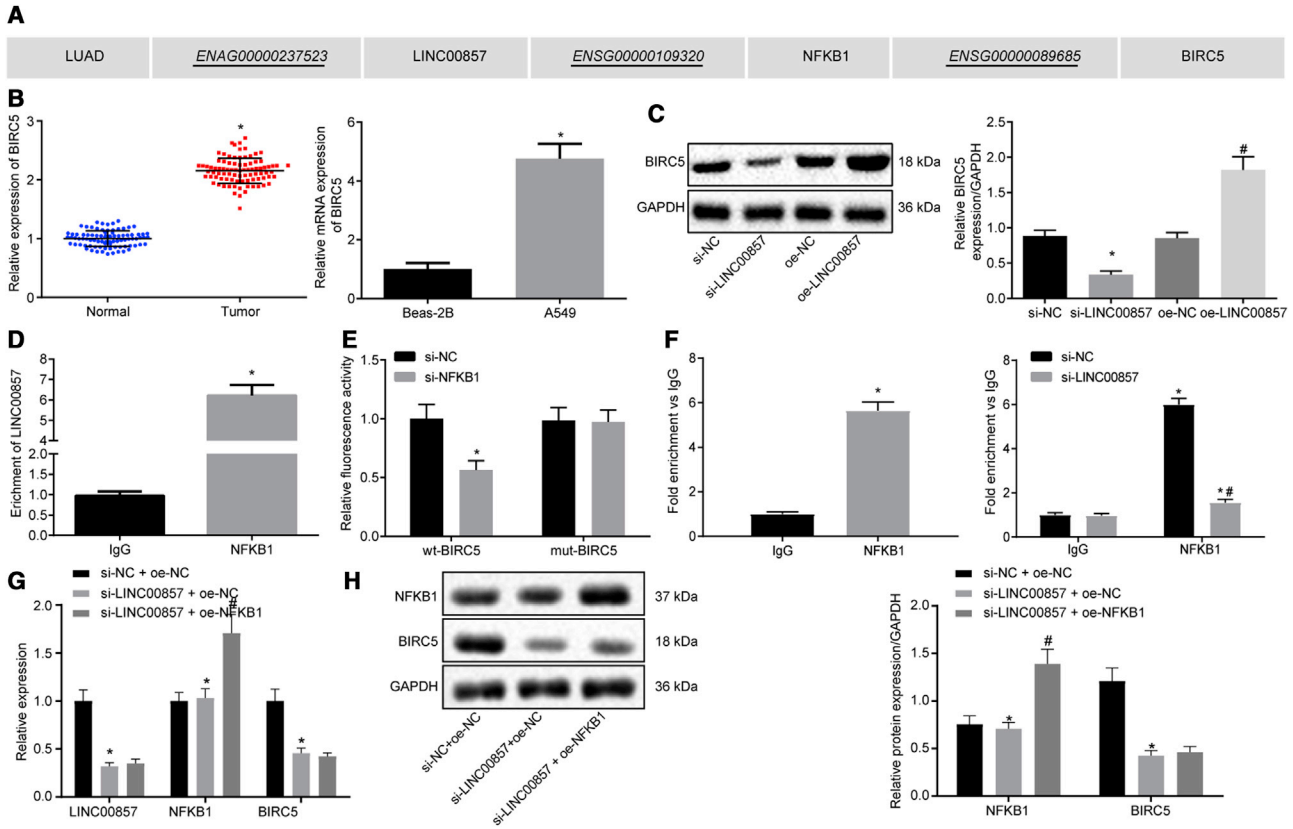

Figure 4. LINC00857 Upregulates BIRC5 Expression by Recruiting NF-κB1

(A) The modulatory role of LINC00857 on LUAD predicted using LncMAP. (B) BIRC5 expression in LUAD tissues (n = 87) and cells determined using qRT-PCR, *p < 0.05 versus normal tissues or Beas-2B cells. (C) BIRC5 protein expression in response to LINC00857 alteration measured by western blot analysis. *p < 0.05 versus si-NC; (D) The binding relationship between LINC00857 and NF-κB1 verified by RIP. *p < 0.05 versus IgG. (E) Dual-luciferase reporter assay was utilized to determine the effect of NF-κB1 on BIRC5, *p < 0.05 versus si-NC. (F) Binding relationship between NFκB1 and BIRC5 detected by ChIP, *p < 0.05 versus IgG; # p < 0.05 versus si-NC. (G) LINC00857, NF-κB1, and BIRC5 expression determined by qRT-PCR, *p < 0.05 versus si-NC + oe-NC, # p < 0.05 versus si-LINC00857 + oe-NC; (H) NF-κB1 and BIRC5 protein expression measured by western blot analysis, * versus si-NC + oe-NC, # p < 0.05 versus si-LINC00857 + oe-NC. Measurement data were expressed as mean ± standard deviation. Paired data conformed to normal distribution and homogeneity of variance were compared using paired t test, while unpaired data were compared by unpaired t test. Differences among multiple groups were analyzed by one-way ANOVA, followed by Tukey's post hoc test. The cell experiment was conducted three times independently.

In conclusion, the present study sheds new light on the mechanism underlying the effects of LINC00857 on radio-sensitivity of LUAD cells (Figure 7). Notably, LINC00857 was upregulated in LUAD cells and tissues, and LINC00857 silencing increased the radiosensitivity of LUAD cells via BIRC5 downregulation. This marker may serve as a therapeutic target for treatment of LUAD in the future. However, further studies should be performed to identify whether LINC00857 can mediate expression of other genes.

MATERIALS AND METHODS

Ethics Statement

All participants signed written informed consents. The current study was conducted under the approval of the Ethics Committee of Shanghai Pulmonary Hospital affiliated with Tongji University School of Medicine and in accordance with the *Declaration of Helsinki*. All animal surgeries were in compliance with the Guide for the Care and Use of Laboratory Animal by the National Institutes of Health.

Study Subjects

A total of 87 tumor tissues were collected from LUAD patients who were admitted in Shanghai Pulmonary Hospital affiliated with Tongji University School of Medicine from January 2015 to January 2016. Among the patients, 56 were males and 31 were females, aged from 20 to 80 years with a mean age of 47 years. There were 10 patients in TNM stage I, 26 patients in stage II, and 51 patients in stage III. The enrolled patients were pathologically or genetically diagnosed as having LUAD without combined tumors of the digestive system or a history of tumors. None of the patients had received chemotherapy or radiotherapy prior to specimen collection. Patients with severe impairment of liver, heart, and kidney function, any history of immune-related diseases, and those who suffered from chronic

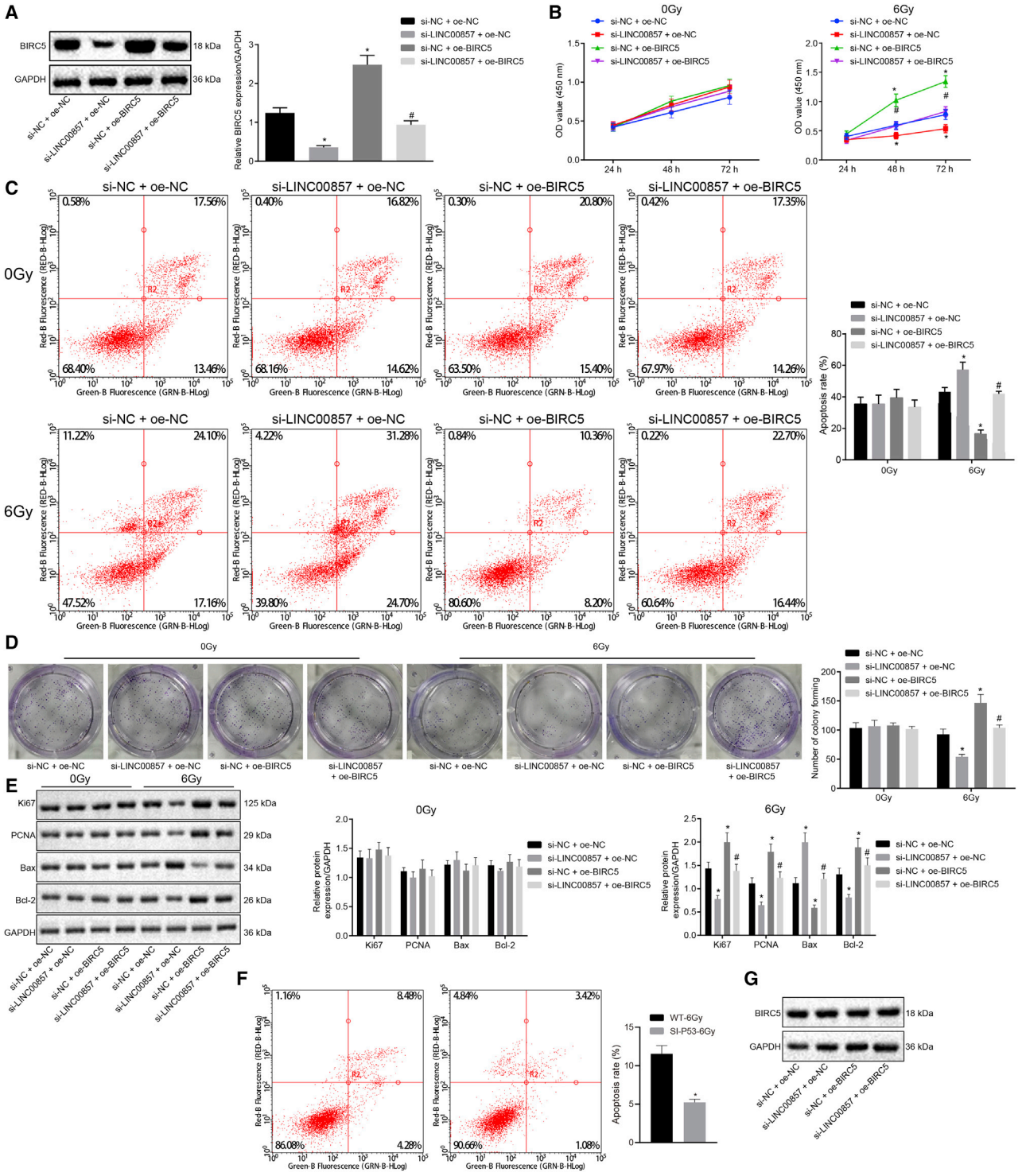

Figure 5. LINC00857-NF-κB1-BIRC5 Triplet Regulated the Radio-Sensitivity in LUAD

The cells used for the following assays were treated with si-NC and oe-NC in combination, both si-LINC00857 and oe-NC in combination, si-LINC00857 and oe-BIRC5 in combination or si-NC and oe-BIRC5 in combination. (A) Transfection efficiency of BIRC5 determined by western blot analysis. (B) LUAD cell viability assessed using CCK-8. (C) LUAD cell apoptosis examined using flow cytometry. (D) Colony-formation capability of LUAD cells. (E) Ki67, PCNA, Bax, and Bcl-2 protein expression measured by

(legend continued on next page)

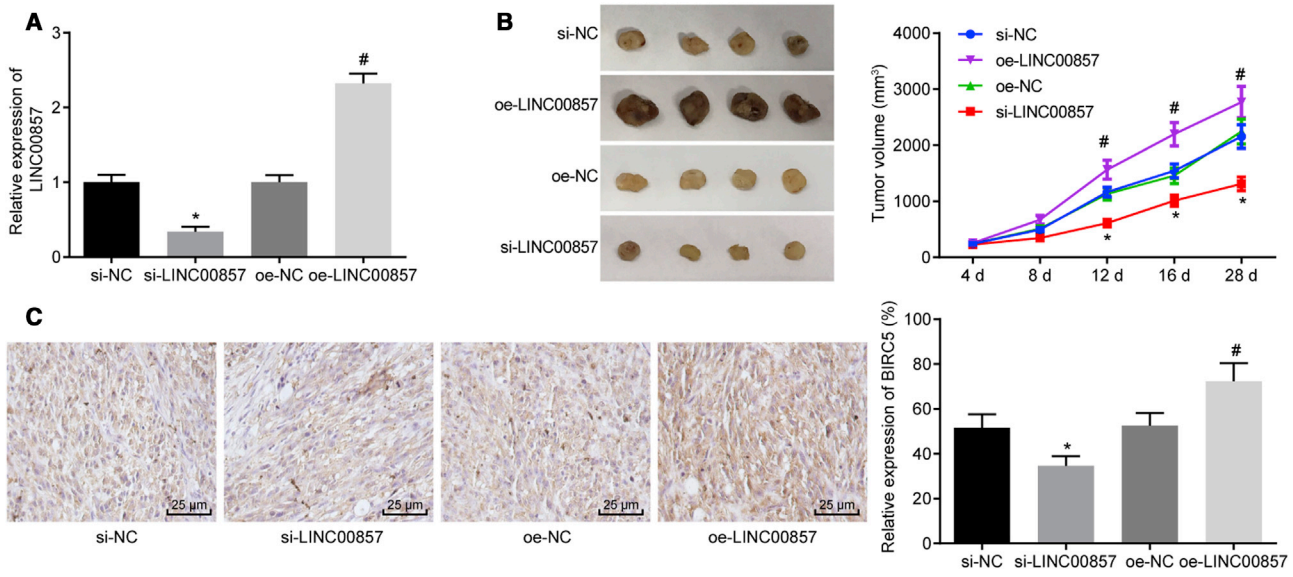

Figure 6. Silencing of LINC00857 Impaired the Progression of LUAD *In Vivo*

(A) qRT-PCR determination of LINC00857 expression in tumor tissues of nude mice. (B) Tumor volume in nude mice monitored at days 4, 8, 12, 16, and 28; n = 10. (C) Immunohistochemical detection of BIRC5 positive rate in tumor tissues (400×); $p < 0.05$, * versus si-NC, # versus oe-NC. Measurement data were expressed as mean ± standard deviation and differences among multiple groups were analyzed by one-way ANOVA, followed by Tukey's post hoc test. Tumor volume at different time points analyzed using repeated-measurement ANOVA, followed by Bonferroni's post hoc test. The experiment was conducted three times independently.

or acute infectious disease were excluded before experimentation. Adjacent normal tissues away from the tumor site were collected as control. No age-based significant difference was observed among multiple groups ($p > 0.05$).

Cell Culture and Lentivirus Construction

Four lung cancer cell lines A549 (LUAD cell line; ATCC CCL-185), H1299 (large cell carcinoma cell line; ATCC CRL-5803), H2444 (ATCC CRL-5945), and H23 (ATCC CRL-5800) as well as the human pulmonary epithelial cell line Beas-2B (ATCC CRL-9609) were obtained from the cell bank of Chinese Academy of Sciences (Shanghai, China). The cell lines presenting with the highest expression of LINC00857 were selected for subsequent experiments. Cells were exposed to different γ-ray irradiation doses (0 Gy, 2.0 Gy, 4.0 Gy, 6.0 Gy, 8.0 Gy, and 10.0 Gy) and then incubated for 24 h. CCK-8 was then adopted to detect LUAD cell viability, following the manufacturer's instructions.

The sequence of LINC00857 was identified in the NCBI databank (https://www.ncbi.nlm.nih.gov/). First, si-LINC00857 (Sigma, St. Louis, MO, USA) was connected to PLKO-Puro (Sigma). After correctly identified by sequencing, the si-LINC00857 plasmid was co-treated with lentivirus vectors psPAX2 or pMD2.G (Addgen, USA) in human embryonic kidney cells (HEK293T), and then lentivirus was collected and purified, followed by detection of viral titers. Next, LUAD cells were seeded to 6-well plates at a density of 3×10^5 cells/well. A549 cells were infected with the lentivirus when cell confluence reached 50%–60%, which was then incubated with 5% CO_2 at 37°C. Cells were collected after 48 h and its infection efficiency was detected prior to further experiment. The sequences of si-LINC00857-1 were F: 5′-GGUAAGGGAAGGUGGAGAAUU-3′, R: 5′-UUCUCCACCUUCCCUUACCUU-3′, and si-LINC00857-2 sequences were F: 5′-GGUAAGGGAAGGUGGAGAAUU-3′, R: 5′-UUGUUCACAGCACAUAGCCUU-3′.

RNA Isolation and Quantification

Total RNA was isolated using TRIzol (Invitrogen, Carlsbad, CA, USA) strictly following the manufacturer's instructions. LINC00857, NF-κB1, and BIRC5 primers were designed and synthesized by Takara Biotechnology (Dalian, China). RNA was reversely transcribed into cDNA using PrimeScript RT reagent kit (RR036A, Takara Biotechnology, Shiga, Japan). According to instructions of in the SYBR Premix Ex Taq II kit (RR820A, Takara Biotechnology, Shiga, Japan), quantitative real-time PCR was then performed using a ABI7500 Real-Time fluorescence quantitative PCR System (7500, ABI, USA). Glyceraldehyde-3-phosphate dehydrogenase (GAPDH) served as internal reference. Fold changes were determined using the relative quantification analysis ($2^{-\delta\delta Ct}$ method; Table 3).

western blot analysis. (F) LUAD cell apoptosis after p53 knockdown under radiation at 6 Gy γ-ray evaluated using flow cytometry. (G) BIRC5 protein expression under radiation at 0, 2, 4, and 6 Gy γ-ray measured by western blot analysis. *$p < 0.05$ versus si-NC + oe-NC, #$p < 0.05$ versus si-LINC00857 + oe-NC; measurement data were expressed as mean ± standard deviation and differences among multiple groups were analyzed by one-way ANOVA, followed by Tukey's post hoc test. OD values at different time points were compared using two-way ANOVA. The cell experiment was conducted three times independently.

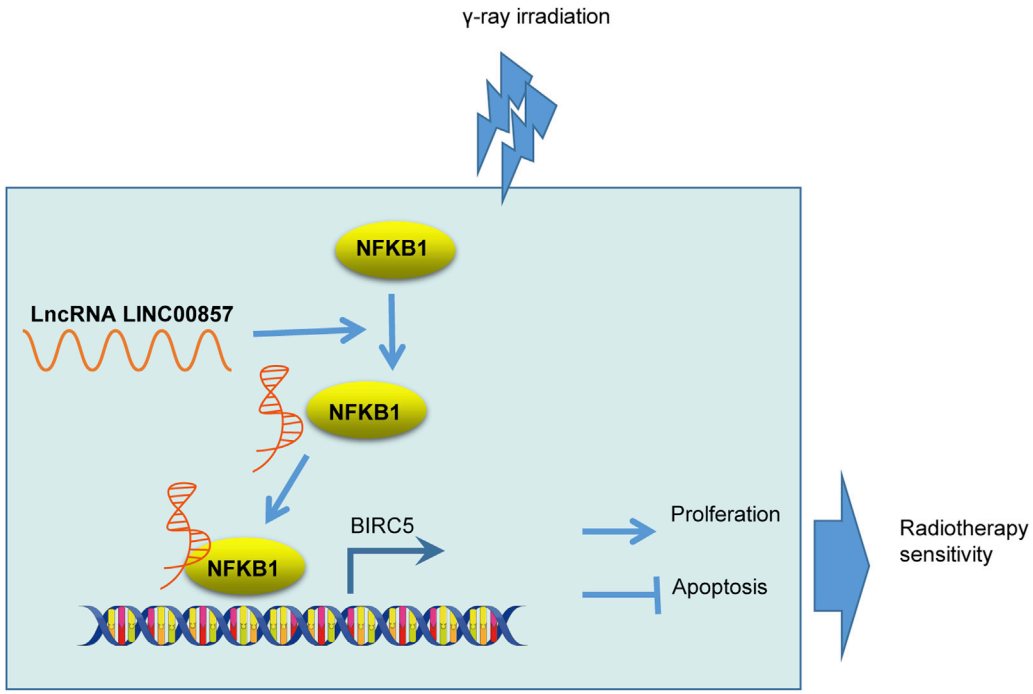

Figure 7. LINC00857 Induces NF-κB1 Enrichment in BIRC5 Promoter thus Elevating BIRC5 Expression, and then BIRC5 Upregulation Contributes to Promoting LUAD Cell Proliferation and Hindering Apoptosis, which Restrains Radiotherapy Sensitivity of LUAD Cells

Western Blot Analysis

The cells were collected and then lysed using radioimmunoprecipitation assay (RIPA) lysis buffer containing phenylmethylsulfonylfluoride (R00013, Beyotime Biotechnology, Shanghai, China), followed by centrifugation at 12,000 rpm at 4°C for 10 min. The supernatant proteins were measured using a bicinchoninic acid (BCA) kit. Next, 50 μg of protein was separated by 10% sodium dodecyl sulfate-polyacrylamide gel electrophoresis and then transferred onto the polyvinylidene fluoride membrane. The membrane was blocked with 5% skim milk at room temperature for 1 h and then incubated at 4°C overnight with the following primary antibodies: NF-κB1 (1:5,000, ab32360), BIRC5 (1 μg/mL, ab469), Ki67 (1:2,000, ab16667), proliferating cell nuclear antigen (PCNA; 1:1,000, ab92552), Bax (1:10,000, ab32503), Bcl-2 (1:10,000, ab59348), and GAPDH (1:1,000, ab181602). All antibodies were purchased from Abcam (Cambridge, UK). After three washes with TBST (5 min each), the membrane was incubated with secondary antibody horseradish peroxidase (HRP)-labeled goat anti-mouse IgG (HA1003, 1:100, Yanhui Biotechnology, Shanghai, China) for 1 h. After development by enhanced chemiluminescence (ECL808-25, Biomiga, San Diego, CA, USA), the protein bands were visualized under a gel imager. With GAPDH as internal reference, the relative protein content was expressed by the ratio of the gray value of the target band to the gray value of GAPDH.

Dual-Luciferase Reporter Gene Assay

The 3′ untranslated region (3′ UTR) of BIRC5 containing WT or MUT NF-κB1 binding site were designed and synthesized by GenePharma Technology (Shanghai, China). The correctly sequenced WT or MUT plasmids were co-transfected with si-NF-κB1 into HEK293T cells, respectively. After 48 h of transfection, cells were then collected and lysed. The luciferase activity was measured using the luciferase assay kit (D0010, Beijing Solarbio Science & Technology, Beijing, China), with a GLomax20/20 Luminometer (Zhongmei Biotechnology, Xian, Shanxi, China) adopted to detect luminance.

RIP Assay

The binding of LINC00857 to NF-κB1 was detected by the RIP kit (Millipore, Billerica, MA, USA). RIPA lysis buffer (P0013B, Beyotime, Shanghai, China) was utilized to lyse cells for 5 min on ice followed by centrifugation at 14,000 rpm at 4°C for 10 min. The supernatant was collected and used as input, while a portion was co-precipitated with antibodies. In brief, 50 μL magnetic beads were extracted and then resuspended with 100 μL RIP wash buffer, followed by incubation with BIRC5 antibody (1 μg/mL, ab469). The magnetic bead-antibody complex was resuspended in 900 μL RIP wash buffer and incubated overnight with 100 μL cell lysate. The magnetic bead-antibody complex was then collected on a magnetic pedestal. The co-precipitated RNA was extracted after detachment by protease K, and then determined by qRT-PCR. IgG (1:100, ab109489) served as NC.

ChIP Assay

Cells were seeded into six-well plates, which were then fixed by 16% formaldehyde. Subsequently, the chromosomal DNA from collected cells was broken by ultrasonic crushing. NF-κB1 antibody (sc-

Table 3. Primer Sequences for qRT-PCR

Genes	Primer Sequence (5′-3′)	
LINC00857	F: CCCCTGCTTCATTGTTTCCC	R: AGCTTGTCCTTCTTGGGTACT
BIRC5	F: GCATGGGTGCCCCGACGTTG	R: GCTCCGGCCAGAGGCCTCAA
NFKB1	F: TCCCCGACCATTGATTGGGCCCGGC	R: TCCCCGACCATTGGGCCCGGC
GAPDH	F: TTGGCATCGTTGAGGGTCT	R: CAGTGGGAACACGGAAAGC

LINC00857, LINCRNA00857; GAPDH, glyceraldehyde-3-phosphate dehydrogenase; qRT-PCR, quantitative reverse transcriptase polymerase chain reaction

365208, 1:1,000, Santa Cruz Biotechnology, Shanghai, China) was added, followed by incubation overnight. Beads were then employed to precipitate the endogenous DNA-protein complex. The DNA-protein complex was de-crosslinked using NaCl (5 mmol/L). The DNA fragments were then collected and the expression of LINC00857 and BIRC5 was determined using qRT-PCR.

Cell Proliferation and Apoptosis Assays

After 48 h of transfection, cells were collected and made into cell suspension (1×10^4 cells/mL) using Dulbecco's modified Eagle's medium supplemented with fetal bovine serum (10%). Cells were seeded into the 96-well plates with 100 μL per well and incubated with 5% CO_2 at 37°C. CCK-8 (10 μL; Sigma, St. Louis, MO, USA) was added into each well after culture for 24 h, 48 h, and 72 h, followed by another 1 h incubation. The optical density (OD) values of each well at 450 nm were measured using a microplate reader (NYW-96M, Beijing Nuyawei, Beijing, China).

Flow cytometry was implemented to determine LUAD cell apoptosis. Cells were inoculated in 96-well plates (2.0×10^3 cells/well), with five replicate wells set for each concentration. Cells were then collected 48 h after X-ray irradiation, followed by centrifugation. Then, binding buffer (200 μL) was added to resuspend the cells, which were mixed with Annexin V-FITC (10 μL; ab14085, Abcam, Cambridge, UK) and incubated for 15 min. Afterward, the cells were mixed with propidium iodide (PI; 5 μL), and then ice-bathed in the dark for 5 min. Cells apoptosis was detected using BD FACSCanto II flow cytometer (Beijing, IMAGE, Beijing, China). Fluorescein isothiocyanate (FITC) was detected upon excitation at 488 nm, while PI was detected at 575 nm.

Colony-Formation Assay

Cells were seeded in agar plates with 800 cells in each plate (75 mm; the proportion of single cells > 95%), followed by addition of 1 mL 3% melted agar (pre-melted in a 65°C water bath). After 48 h of incubation, the cells were washed with pH 6.8 phosphate buffer and then fixed by methanol for 20 min. Giemse was utilized to stain cells for 20 min. Finally, colonies containing more than 20 cells were counted under the microscope.

Tumor Xenografts in Nude Mice

A total of 40 male BALB/c-nu/nu nude mice (aged 6 weeks; weighing from 18 to 22 g with the mean weight of 20 g) were purchased from Shanghai SLAC Biological Technology (Shanghai, China). The nude mice were randomly grouped into: si-NC, si-LINC00857, oe-NC, and oe-LINC00857 groups (mice injected with cells infected with lentivirus expressing si-NC, si-LINC00857, oe-NC, and oe-LINC00857 plasmids, respectively). In brief, the cells were infected with lentivirus to obtain stably infected cell lines. The cell suspension was inoculated into the mice. The mice were exposed to radiation (6 Gy γ-ray) after tumor formation.[34] The length and width of the tumors were detected using Vernier caliper and tumor volume was calculated 3 times with the following formula: TV (tumor volume) = $1/2 \times a \times b^2$, in which a referred to short diameter and b the long diameter. Nude mice were euthanized on the 28th d and tumors were extracted. The tumor tissues (5 in each group) were weighed, fixed, paraffin-embedded, and sliced into sections.

Immunohistochemistry

Tumor tissues isolated from the nude mice were paraffin-embedded, sectioned, and dehydrated, followed by dewaxing using xylene I and II for 10 min separately. The tumor samples were dehydrated with gradient alcohol (100%, 95%, 80%, and 70%) for 2 min respectively, and then immersed in 3% H_2O_2 for 10 min, followed by antigen retrieval under high pressure for 90 s. Bovine serum albumin (BSA; 5%) was added to block the sections and incubated at 37°C for 30 min. Subsequently, the samples were incubated with the primary polyclonal antibody rabbit anti-mouse BIRC5 (1: 250, ab469) at 4°C overnight. Biotinylated mouse anti-goat IgG (50 μL; RXE0155; Rongchuang Data, Technology, Beijing, China) was then added and incubated at 37°C for 30 min. After development by diaminobenzidine (DAB) and staining with hematoxylin for 5 min, five fields in each section were randomly selected and photographed under a microscope. PBS was used as the NC of the primary antibody, and the positive cells in which cytoplasm was stained yellow-brown were counted.

Statistical Analysis

All data were processed and analyzed using SPSS 21.0 statistical software (IBM, Armonk, NY, USA). Measurement data were expressed as mean ± standard deviation. Paired data conforming to normal distribution and homogeneity of variance were compared using paired t test, while unpaired t test was adopted to compare the unpaired data. Differences among multiple groups were analyzed by one-way analysis of variance (ANOVA), followed by Tukey's post hoc test.

Tumor volumes at different time points were compared using repeated-measurement ANOVA, followed by Bonferroni's post hoc test. OD values at different time points were compared using two-way ANOVA. Kaplan-Meier method was applied to calculate the survival rate, and Log-rank test was performed to analyze the single factor. $p < 0.05$ was considered statistically significant.

SUPPLEMENTAL INFORMATION

Supplemental Information can be found online at https://doi.org/10.1016/j.omtn.2020.09.020.

AUTHOR CONTRIBUTIONS

F.H., S.Y., S.C., and W.W. designed the study. F.H., X.H., S.Y., and D.H. collated the data, carried out data analyses, and produced the initial draft of the manuscript. W.W., D.H., and S.C. contributed to drafting the manuscript. All authors read and approved the final manuscript.

CONFLICTS OF INTEREST

The authors declare no competing interests.

ACKNOWLEDGMENTS

We would like to thank our researchers for their hard work and reviewers for their valuable advice.

REFERENCES

1. Cancer Genome Atlas Research Network (2014). Comprehensive molecular profiling of lung adenocarcinoma. Nature *511*, 543–550.
2. Cassidy, R.J., Zhang, X., Patel, P.R., Shelton, J.W., Escott, C.E., Sica, G.L., Rossi, M.R., Hill, C.E., Steuer, C.E., Pillai, R.N., et al. (2017). Next-generation sequencing and clinical outcomes of patients with lung adenocarcinoma treated with stereotactic body radiotherapy. Cancer *123*, 3681–3690.
3. Kim, K.T., Lee, H.W., Lee, H.O., Kim, S.C., Seo, Y.J., Chung, W., Eum, H.H., Nam, D.H., Kim, J., Joo, K.M., and Park, W.Y. (2015). Single-cell mRNA sequencing identifies subclonal heterogeneity in anti-cancer drug responses of lung adenocarcinoma cells. Genome Biol. *16*, 127.
4. Esteller, M. (2011). Non-coding RNAs in human disease. Nat. Rev. Genet. *12*, 861–874.
5. Gupta, R.A., Shah, N., Wang, K.C., Kim, J., Horlings, H.M., Wong, D.J., Tsai, M.C., Hung, T., Argani, P., Rinn, J.L., et al. (2010). Long non-coding RNA HOTAIR reprograms chromatin state to promote cancer metastasis. Nature *464*, 1071–1076.
6. Zhou, J., Xiao, H., Yang, X., Tian, H., Xu, Z., Zhong, Y., Ma, L., Zhang, W., Qiao, G., and Liang, J. (2018). Long noncoding RNA CASC9.5 promotes the proliferation and metastasis of lung adenocarcinoma. Sci. Rep. *8*, 37.
7. Zhang, M., Gao, C., Yang, Y., Li, G., Dong, J., Ai, Y., Chen, N., and Li, W. (2018). Long Noncoding RNA CRNDE/PRC2 Participated in the Radiotherapy Resistance of Human Lung Adenocarcinoma Through Targeting p21 Expression. Oncol. Res. *26*, 1245–1255.
8. Wang, L., He, Y., Liu, W., Bai, S., Xiao, L., Zhang, J., Dhanasekaran, S.M., Wang, Z., Kalyana-Sundaram, S., Balbin, O.A., et al. (2016). Non-coding RNA LINC00857 is predictive of poor patient survival and promotes tumor progression via cell cycle regulation in lung cancer. Oncotarget *7*, 11487–11499.
9. Wang, L., Cao, L., Wen, C., Li, J., Yu, G., and Liu, C. (2020). LncRNA LINC00857 regulates lung adenocarcinoma progression, apoptosis and glycolysis by targeting miR-1179/SPAG5 axis. Hum. Cell *33*, 195–204.
10. Long, Y., Wang, X., Youmans, D.T., and Cech, T.R. (2017). How do lncRNAs regulate transcription? Sci Adv *3*, eaao2110.
11. Knauer, S.K., Unruhe, B., Karczewski, S., Hecht, R., Fetz, V., Bier, C., Friedl, S., Wollenberg, B., Pries, R., Habtemichael, N., et al. (2013). Functional characterization of novel mutations affecting survivin (BIRC5)-mediated therapy resistance in head and neck cancer patients. Hum. Mutat. *34*, 395–404.
12. Knizhnik, A.V., Kovaleva, O.B., Laktionov, K.K., Mochal'nikova, V.V., Komel'kov, A.V., Chevkina, E.M., and Zborovskaia, I.B. (2011). [Arf6, RalA and BIRC5 protein expression in non small cell lung cancer]. Mol. Biol. (Mosk.) *45*, 307–315.
13. Yu, X., Zhang, Y., Wu, B., Kurie, J.M., and Pertsemlidis, A. (2019). The miR-195 Axis Regulates Chemoresistance through TUBB and Lung Cancer Progression through BIRC5. Mol. Ther. Oncolytics *14*, 288–298.
14. Ni, K.W., and Sun, G.Z. (2019). The identification of key biomarkers in patients with lung adenocarcinoma based on bioinformatics. Math. Biosci. Eng. *16*, 7671–7687.
15. Cartwright, T., Perkins, N.D., and L Wilson, C. (2016). NFKB1: a suppressor of inflammation, ageing and cancer. FEBS J. *283*, 1812–1822.
16. Ferlay, J., Shin, H.R., Bray, F., Forman, D., Mathers, C., and Parkin, D.M. (2010). Estimates of worldwide burden of cancer in 2008: GLOBOCAN 2008. Int. J. Cancer *127*, 2893–2917.
17. Balça-Silva, J., Sousa Neves, S., Gonçalves, A.C., Abrantes, A.M., Casalta-Lopes, J., Botelho, M.F., Sarmento-Ribeiro, A.B., and Silva, H.C. (2012). Effect of miR-34b overexpression on the radiosensitivity of non-small cell lung cancer cell lines. Anticancer Res. *32*, 1603–1609.
18. Xie, W., Yuan, S., Sun, Z., and Li, Y. (2016). Long noncoding and circular RNAs in lung cancer: advances and perspectives. Epigenomics *8*, 1275–1287.
19. Arun, G., Diermeier, S., Akerman, M., Chang, K.C., Wilkinson, J.E., Hearn, S., Kim, Y., MacLeod, A.R., Krainer, A.R., Norton, L., et al. (2016). Differentiation of mammary tumors and reduction in metastasis upon Malat1 lncRNA loss. Genes Dev. *30*, 34–51.
20. Li, Y., Wang, Z., Nair, A., Song, W., Yang, P., Zhang, X., and Sun, Z. (2017). Comprehensive Profiling of lincRNAs in Lung Adenocarcinoma of Never Smokers Reveals Their Roles in Cancer Development and Prognosis. Genes (Basel) *8*, 321.
21. Zhang, N., and Jiang, W. (2019). Long non-coding RNA DANCR promotes HMGA2-mediated invasion in lung adenocarcinoma cells. Oncol. Rep. *41*, 1083–1090.
22. Wang, H., Zhang, X., Wang, L., Zheng, G., Du, L., Yang, Y., Dong, Z., Liu, Y., Qu, A., and Wang, C. (2014). Investigation of cell free BIRC5 mRNA as a serum diagnostic and prognostic biomarker for colorectal cancer. J. Surg. Oncol. *109*, 574–579.
23. Cao, Y., Zhu, W., Chen, W., Wu, J., Hou, G., and Li, Y. (2019). Prognostic Value of BIRC5 in Lung Adenocarcinoma Lacking EGFR, KRAS, and ALK Mutations by Integrated Bioinformatics Analysis. Dis. Markers *2019*, 5451290.
24. Han, X., Liu, M., Wang, S., Lv, G., Ma, L., Zeng, C., and Shi, Y. (2015). An Integrative Analysis of the Putative Gefitinib-resistance Related Genes in a Lung Cancer Cell Line Model System. Curr. Cancer Drug Targets *15*, 423–434.
25. Lu, B., Mu, Y., Cao, C., Zeng, F., Schneider, S., Tan, J., Price, J., Chen, J., Freeman, M., and Hallahan, D.E. (2004). Survivin as a therapeutic target for radiation sensitization in lung cancer. Cancer Res. *64*, 2840–2845.
26. Tennstedt, P., Köster, P., Brüchmann, A., Mirlacher, M., Haese, A., Steuber, T., Sauter, G., Huland, H., Graefen, M., Schlomm, T., et al. (2012). The impact of the number of cores on tissue microarray studies investigating prostate cancer biomarkers. Int. J. Oncol. *40*, 261–268.
27. Li, Y., Li, L., Li, B., Wu, Z., Wu, Y., Wang, Y., Jin, F., Li, D., Ma, H., and Wang, D. (2016). Silencing of ataxia-telangiectasia mutated by siRNA enhances the in vitro and in vivo radiosensitivity of glioma. Oncol. Rep. *35*, 3303–3312.
28. Jiang, H., Zhao, P., Feng, J., Su, D., and Ma, S. (2014). Effect of Paris saponin I on radiosensitivity in a gefitinib-resistant lung adenocarcinoma cell line. Oncol. Lett. *7*, 2059–2064.
29. Nakanishi, C., and Toi, M. (2005). Nuclear factor-kappaB inhibitors as sensitizers to anticancer drugs. Nat. Rev. Cancer *5*, 297–309.
30. Chen, W., Li, Z., Bai, L., and Lin, Y. (2011). NF-kappaB in lung cancer, a carcinogenesis mediator and a prevention and therapy target. Front. Biosci. *16*, 1172–1185.

31. Li, F., and Sethi, G. (2010). Targeting transcription factor NF-kappaB to overcome chemoresistance and radioresistance in cancer therapy. Biochim. Biophys. Acta *1805*, 167–180.

32. Arora, H., Qureshi, R., Jin, S., Park, A.K., and Park, W.Y. (2011). miR-9 and let-7g enhance the sensitivity to ionizing radiation by suppression of NFκB1. Exp. Mol. Med. *43*, 298–304.

33. Wang, R., Peng, S., Zhang, X., Wu, Z., Duan, H., Yuan, Y., and Wang, W. (2019). Inhibition of NF-κB improves sensitivity to irradiation and EGFR-TKIs and decreases irradiation-induced lung toxicity. Int. J. Cancer *144*, 200–209.

34. Ji, C., Xu, Q., Guo, L., Wang, X., Ren, Y., Zhang, H., Zhu, W., Ming, Z., Yuan, Y., Ren, X., et al. (2018). eEF-2 Kinase-targeted miR-449b confers radiation sensitivity to cancer cells. Cancer Lett. *418*, 64–74.

OMTN, Volume *22*

Supplemental Information

Silencing of lncRNA LINC00857 Enhances BIRC5-Dependent Radio-Sensitivity of Lung Adenocarcinoma Cells by Recruiting NF-κB1

Fushi Han, Shusong Yang, Wei Wang, Xinghong Huang, Dongdong Huang, and Shuzhen Chen

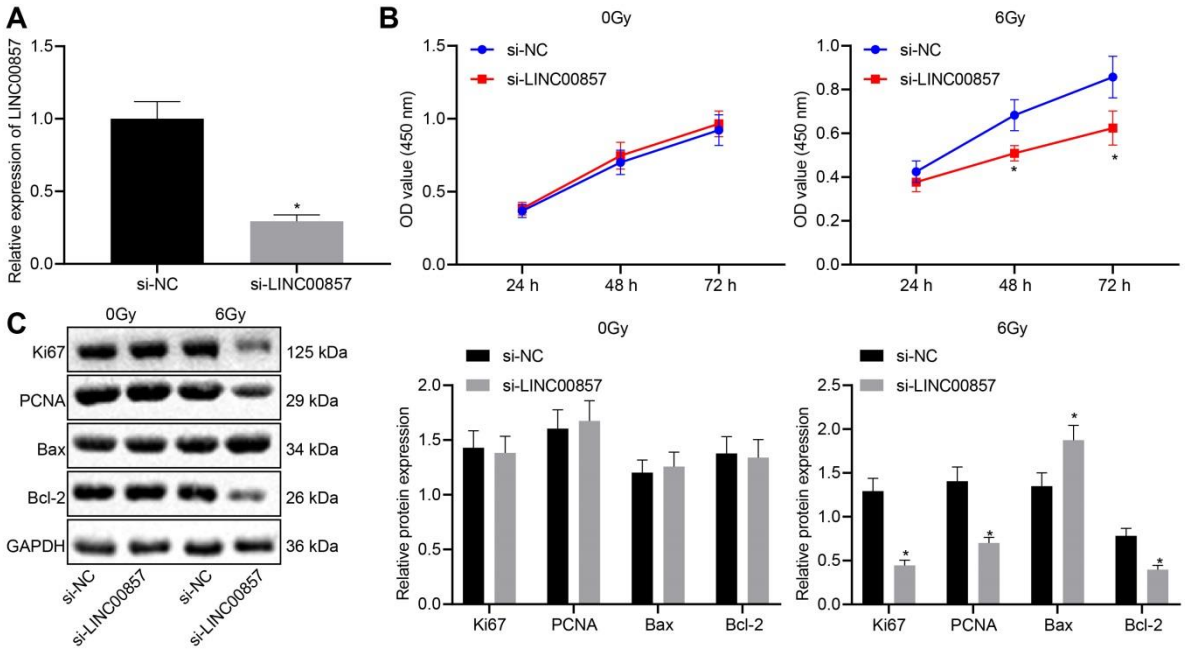

Supplementary Figure 1. LINC00857 knockdown enhanced radio-sensitivity of H2444 cells. A, Transfection efficiency measured by RT-qPCR. B, Viability of H2444 cells after LINC00857 knockdown tested using CCK-8. C, Western blot analysis of Ki67, PCNA, Bax and Bcl-2 protein expression in H2444 cells after LINC00857 knockdown. * $p < 0.05$ *vs.* si-NC; measurement data were expressed as mean ± standard deviation and analyzed by unpaired *t* test. OD values at different time points were compared using two-way ANOVA. The cell experiments were conducted three times independently.